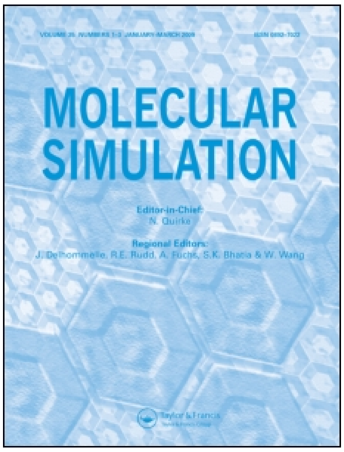

Molecular Simulation
Publication details, including instructions for authors and subscription information:
http://www.informaworld.com/smpp/title~content=t713644482

MD Simulation of the Self-diffusion Coefficient and Dielectric Properties of Expanded Liquids—I. Methanol and Carbon Dioxide Mixtures

Tsutomu Aida[a]; Hiroshi Inomata[a]
[a] Research Center of Supercritical Fluid Technology, Tohoku University, Sendai, Japan

To cite this Article Aida, Tsutomu and Inomata, Hiroshi(2004) 'MD Simulation of the Self-diffusion Coefficient and Dielectric Properties of Expanded Liquids—I. Methanol and Carbon Dioxide Mixtures', Molecular Simulation, 30: 6, 407 — 412

To link to this Article: DOI: 10.1080/0892702042000198828

URL: http://dx.doi.org/10.1080/0892702042000198828

Molecular Simulation, Vol. 30 (6), 15 May 2004, pp. 407–412

Taylor & Francis
Taylor & Francis Group

MD Simulation of the Self-diffusion Coefficient and Dielectric Properties of Expanded Liquids—I. Methanol and Carbon Dioxide Mixtures

TSUTOMU AIDA[†] and HIROSHI INOMATA*

Research Center of Supercritical Fluid Technology, Tohoku University, Aramaki Aza Aoba-07, Aoba-ku, Sendai 980-8579, Japan

(Received July 2003; In final form January 2004)

Methanol can dissolve considerable amounts of CO_2 under pressure. When this occurs, viscosity decreases and volume increases, which is a typical feature of expanded liquids. In this study, molecular dynamics (MD) simulations were conducted for methanol and CO_2 mixtures at 50°C and high pressures to explore features of the expanded liquid state in terms of solution structure. Radial distribution function for methanol–methanol molecules showed that methanol molecules formed hydrogen bonds and nearest hydrogen bonds distance was not changed. The self-diffusion coefficients of both methanol and CO_2 were found to decrease monotonically from the pure CO_2 side and then not to change appreciably at methanol mole fractions higher than about 0.5. It should also be noted that the simulation results could qualitatively present the dielectric spectroscopy results reported in the literature. These results showed that methanol molecules make hydrogen bond networks and hydrogen bond networks surrounded CO_2 molecules at mole fractions higher than about 0.5. Further addition of CO_2 into methanol caused the hydrogen bond networks to break up and to form smaller hydrogen bond aggregates.

Keywords: Molecular dynamics; Methanol–CO_2 molecules; Simulation; Hydrogen bond networks

INTRODUCTION

Mutual solubility between methanol and CO_2 is very low at atmospheric pressure around room temperature. However, at pressures above 10 MPa, CO_2 and methanol form homogenous mixtures over the entire range of compositions [1]. Especially near the mixture critical point, methanol can be considered to be in an expanded state. Expanded liquids have much attention as solvents for high performance liquid chromatography [2], metal ion extraction [3], polymerizations [4] and polymer coating [5] due to the highly adjustable properties such as viscosity and solubility.

Experimental research has been performed by various researchers to study features of expanded liquid solutions. Reighard *et al.* studied the phase behavior of methanol and CO_2 mixtures at 25–100°C, 3–20 MPa [6]. They found that the range of methanol mole fractions (X_{MeOH}) 0.5–0.7, where high pressures are required to form and maintain a single phase at several temperatures. Smith *et al.* reported dielectric spectra of methanol and CO_2 mixtures at 40–50°C and 11 MPa [7]. They found that the dielectric constant increased with increasing X_{MeOH} and the dielectric relaxation time exhibited a maximum around X_{MeOH} of 0.8 over the temperature range of 40–50°C. They hypothesized that CO_2 initially entered into the methanol hydrogen bond networks and inhibited dipole movement through strong dipole–quadrupole interactions that were later weakened at higher CO_2 mole fractions.

In this work, our objective was to elucidate some of the mechanistic features of the results reported by Smith *et al.* [7] with molecular dynamics (MD) simulations of methanol and CO_2 mixtures, and to examine some of the solution structural features of the expanded liquid state of methanol in terms of the radial distribution function (RDF), self-diffusion coefficient and dielectric properties.

SIMULATION DETAILS

The potentials used in this work were both 3-sites flexible models for methanol [8] and CO_2 [9].

---

*Corresponding author. Tel.: +81-22-217-7283. Fax: +81-22-217-7247. E-mail: inomata@scf.che.tohoku.ac.jp

[†] E-mail: aidajpn@scf.che.tohoku.ac.jp

ISSN 0892-7022 print/ISSN 1029-0435 online © 2004 Taylor & Francis Ltd
DOI: 10.1080/0892702042000198828

TABLE I LJ and Coulombic potential parameters for methanol [8] and CO_2 [9] molecules

Molecule	*Group*	*ε (kJ/mol)*	*σ (Å)*	*q (e)*
Methanol	CH_3	1.2307	3.7300	0.2650
	O	0.7539	3.0645	− 0.7000
	H	0.0100	0.9000	0.4350
CO_2	C	0.2410	3.1260	0.5100
	O	0.6906	3.2640	− 0.2550

Both models can prove liquid and supercritical state. The three sites for methanol are oxygen (O), hydrogen (H) and methyl group ($-CH_3$). Both flexible models can be represented as a sum of intra- and inter-molecular potentials. The intramolecular potential used the angular form of Toukan–Rahman (TR) potential [10]. The intermolecular potential used a Lennard–Jones (LJ) 12–6 potential and a Coulombic potential. We determined LJ parameters for interactions between methanol and CO_2 molecules via [11]

$$\varepsilon_{12} = \left(\frac{2\sqrt{I_1 I_2}}{I_1 + I_2}\right)\left(\frac{2^6 \times \sigma_1^3 \sigma_2^3}{(\sigma_1 + \sigma_2)^6}\right)\sqrt{\varepsilon_1 \varepsilon_2} \tag{1}$$

$$\sigma_{12} = \frac{1}{2}(\sigma_1 + \sigma_2) \tag{2}$$

where I is the ionized potential. We calculated ionized potential by MOPAC6, $I_{CH_3OH} = 46.77\,\mathrm{kJ/mol}$ and $I_{CO_2} = 55.50\,\mathrm{kJ/mol}$. Tables I and II show the LJ and Coulombic potential parameters of methanol and CO_2 that were taken from Refs. [8,9].

All simulations were performed with NVT-ensembles for several methanol mole fractions. We wanted to study methanol and CO_2 mixtures at 50°C and 11 MPa for allowing us to compare the simulation results with the experimental result studied by Smith *et al.* [7]. The number of molecules was 500. The simulation volume of each composition was determined for density, which was set to correspond to 11 MPa at 50°C from the experimental data [12]. The values used in this work are reproduced in Table III. It should be noted that the densities in Table III exhibit a maximum when plotted against composition. The temperature was initially (~60 ps) controlled by momentum scaling and afterwards (60 ps ~) by Nosè-Hoover thermostat for computational stability. These determined conditions were nearly caused at 50°C and 11 MPa. The equation of motion was integrated using the velocity Verlet technique with multiple time scale algorithm by Tuckerman *et al.* [13]. The time step was 0.2 fs for intra-dynamics and 1 fs for inter-dynamics. Statistical sampling of the simulation was done for 3000 ps after 100 ps equilibration.

TABLE II Intramolecular potential parameters for methanol [8] and CO_2 [9] molecules

Molecule			
Methanol	Bond (Å)	CH_3-O	1.430
		$O-H$	0.945
	Angle (°)	CH_3-O-H	108.5
CO_2	Bond (Å)	$C=O$	1.149
	Angle (°)	$O=C=O$	180.0

TABLE III Simulation conditions for methanol and CO_2 mixtures at 50°C, 11 MPa

X_{MeOH} (-)	*Experimental density [12] (kg/m³)*	*Simulation density (kg/m³)*	*Length of simulation cell (Å)*	*Simulation molar density (×10⁴ mol/m³)*
1.0	774	785	32.36	2.453
0.9	794	805	32.49	2.425
0.8	808	819	32.68	2.381
0.7	819	830	32.91	2.332
0.6	816	827	33.31	2.247
0.5	808	819	33.78	2.216
0.4	794	805	34.33	2.054
0.3	765	776	35.10	1.921
0.2	707	717	36.39	1.724

PROPERTY EVALUATION

The RDF was calculated by the following equation:

$$g(r) = \frac{V}{N}\frac{\Delta n(r)}{4\pi r^2 \Delta r} \tag{3}$$

where V is the volume of the simulation system, N is the number of all molecules in the simulation system and $\Delta n(r)$ is the number of the molecules in $4\pi r^2 \Delta r$.

The self-diffusion coefficient was calculated by the mean square displacement (MSD) using the Einstein relationship [14]:

$$D = \lim_{t \to \infty} \frac{1}{6t}\left\langle [\vec{r}(t) - \vec{r}(0)]^2 \right\rangle \tag{4}$$

where $\vec{r}$ is the position vector of molecules, t is the time and $\langle\,\rangle$ means the ensemble average.

The dielectric properties, the static dielectric constant (ε_0) and the relaxation time (τ_0) were calculated as follows [15]. The static dielectric constant was calculated by the following equation:

$$\varepsilon_0 = 1 + \frac{4\pi}{3Nk_B T}\left\langle \{\Phi_{MM}(0)\}^2 \right\rangle \tag{5}$$

where k_B is the Boltzmann constant and T is the absolute temperature. The time correlation function (TCF) of system dipole was defined and calculated from:

$$\Phi_{MM}(t) = \left\langle \vec{M}(t) \cdot \vec{M}(0) \right\rangle \tag{6}$$

where $\vec{M}$ is the sum of all molecular dipole vectors in the system. For the case that TCF can be described by an exponential function, a Debye process can describe the dielectric relaxation. The relaxation time (τ_0) was determined from the following equation:

$$\Phi_{MM}(t) = A \exp\left(-\frac{t}{\tau_0}\right) \tag{7}$$

We calculated relaxation time by average value of separating the 3000 ps simulation time into 50 ps sequent. The simulation data was compared with the experimental dielectric properties measurements [7].

RESULTS AND DISCUSSION

Pure Methanol

Figure 1 shows the methanol oxygen–oxygen RDF and Fig. 2 shows methanol oxygen–hydrogen RDF at X_{MeOH} of 1.0 together with another simulation data at 25°C [16,17]. In Fig. 1, the position at the first maximum peak occurred at 2.8 Å and that of the first minimum can be seen at 3.4 Å In Fig. 2, the position at the first maximum peak occurred at 1.8 Å and that of the first minimum occurred at 2.6 Å. Yamaguchi *et al.* studied pure methanol by empircial potential structure refinement simulation using the *H1* potential model [18] at 25°C. In our study, the positions of the oxygen–oxygen and oxygen–hydrogen RDFs were agreed with their results. Other simulation results of RDFs, Handgraaf *et al.* by *ab initio* simulation at 20°C [19] and Kosztolanyi *et al.* by MD simulation using OPLS potential model [20] at 25°C [21] also gave similar positions for the first maximum and first minimum peak. Those authors proposed that the positions of first maximum and minimum peak by oxygen–oxygen and oxygen–hydrogen RDF were strong related to hydrogen bonding. It should be noted Methanol molecules can form hydrogen bond at 50°C and 11 MPa and hydrogen bond length did not change at 20, 25 and 50°C.

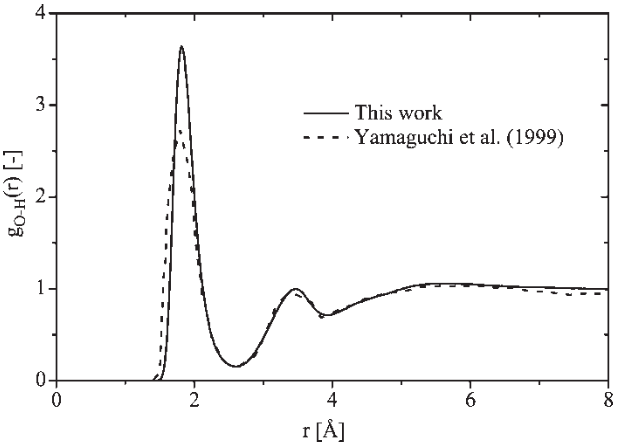

FIGURE 2 Methanol oxygen–hydrogen RDF at X_{MeOH} of 1.0 at 50°C (line) with the data at 25°C studied by Yamaguchi *et al.* [16,17] (broken line). See Table III for densities.

Methanol and CO_2 Mixtures

Figure 3 shows the methanol oxygen–oxygen RDF and Fig. 4 shows the methanol oxygen–hydrogen RDF at X_{MeOH} of 0.8, 0.6, 0.4 and 0.2, respectively. In Figs. 3 and 4, the distribution was sharp with decreasing X_{MeOH}. The positions at the first maximum peak and first minimum peak did not change so much with X_{MeOH}. These indicated that the methanol hydrogen bond pairs seemed not to be affected by CO_2 molecules.

In Fig. 3, the methanol oxygen–oxygen RDF peak position of second maximum and minimum seemed not to change with increasing X_{MeOH}. The position of the second minimum peak was almost constant at 6.0 Å. The number of

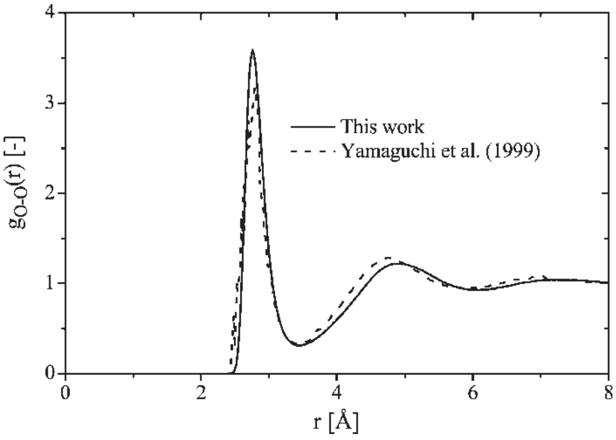

FIGURE 1 Methanol oxygen–oxygen RDF at X_{MeOH} of 1.0 at 50°C (line) with the data at 25°C studied by Yamaguchi *et al.* [15,16] (broken line). See Table III for densities.

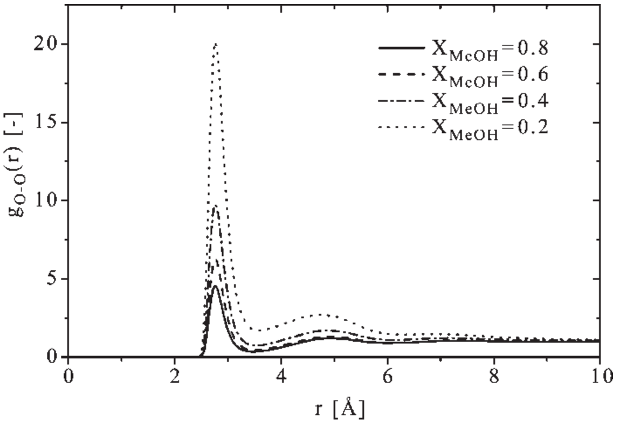

FIGURE 3 Methanol oxygen–oxygen RDF at X_{MeOH} of 0.8, 0.6, 0.4 and 0.2 at 50°C. See Table III for densities.

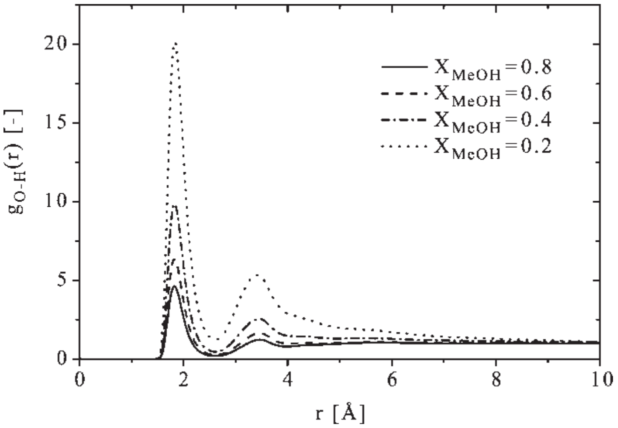

FIGURE 4 Methanol oxygen–hydrogen RDF at X_{MeOH} of 0.8, 0.6, 0.4 and 0.2 at 50°C. See Table III for densities.

methanol molecules $n(r)$ within the distance r were calculated from methanol oxygen–oxygen RDF by integrating Eq. (3) via:

$$n(r) = 4\pi \frac{N}{V}\int_0^r g_{O-O}(r) r^2\, dr \tag{8}$$

The first shell could be defined from 0 to 3.4 Å and the second shell from 0 to 6.0 Å from the RDF.

Figure 5 shows a plot of $n(r)$ in the first and second shells versus X_{MeOH}. In the first shell, $n(r)$ was almost 2 at X_{MeOH} more than 0.5. At X_{MeOH} less than 0.5, $n(r)$ was slightly decreased with decreasing X_{MeOH}. This means that a center methanol molecule probably makes hydrogen bonds with two other methanol molecules at X_{MeOH} more than 0.5. At X_{MeOH} less than 0.5, a center methanol molecule still seemed to form hydrogen bonds, but could not make hydrogen bonds rigidly with two other methanol molecules. We thought CO_2 might start to affect the hydrogen bond pairs and methanol hydrogen bond networks around X_{MeOH} of 0.5. On the other hand the second shell, $n(r)$ seemed to decrease monotonically with decreasing X_{MeOH}. The number of methanol molecules in the simulation system decreased with decreasing X_{MeOH} and $n(r)$ decreased in the second shell. This shows that the center methanol molecule had little effect on the second shell structure that had generally weak interactions.

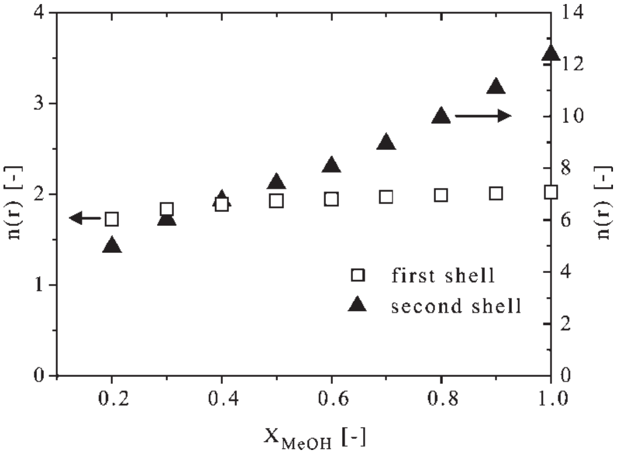

FIGURE 5 Integrated average numbers of molecules in first and second shells of methanol oxygen–oxygen RDF from Eq. (8) as a function of methanol mole fraction. See Table III for densities.

Figure 6 shows simulation results for the self-diffusion coefficients of methanol and CO_2. Both the self-diffusion coefficients decreased gradually with increasing X_{MeOH}. However, around X_{MeOH} of 0.5, there appeared to be a transition in the slope. Both self-diffusion coefficients showed small changes with increasing X_{MeOH}, especially the methanol diffusivity values at X_{MeOH} more than 0.5. This behavior seemed to be similar to that of the first shell $n(r)$ in Fig. 5. In Table III, the molar density increases with increasing X_{MeOH}. This might cause the collision frequency of molecules to increase and lower the self-diffusion coefficients for higher X_{MeOH}. It should also be noted that the CO_2 diffusivity approaches that of methanol at higher X_{MeOH}, which suggests that CO_2 molecules tend to move with methanol molecules in these compositions. From these results, we concluded that CO_2 dissolution into methanol did not seem to have a large effect on the methanol hydrogen bond networks as a small amount of CO_2 was added to the methanol solvent. Further increases in the number of CO_2 molecules in the system at X_{MeOH} less than 0.5, however, lead to the result that the system could not maintain the integrity of the hydrogen bonding networks.

Figure 7 shows simulation results for the static dielectric constant from Eq. (7) together with the experimental data [7]. Although fairly large discrepancies exist between experimental and simulated values, it can be seen that the simulation could represent the trend of the static dielectric constant with composition. The static dielectric constant increased with increasing X_{MeOH}. Increasing the number of methanol molecules caused an increase in the total dipole moment $\vec{M}(0)$ of the system.

The relaxation time evaluated from dipole time correlation and Eq. (5) was plotted against X_{MeOH} together with the experimental data [7] in Fig. 8. The tendency between experimental and simulated values seemed to be similar if the simulation results at $X_{MeOH} = 0.5$ and 0.9 were excluded. We calculated relaxation time by average value of 60 segments of 50 ps simulation segment. If we excluded some points of large dispersion, the relaxation time was decreased and the tendency was similar. We noted that the data did not show a monotonic increase of τ_0 with increasing X_{MeOH}, which is evidence for the possible existence of a maximum τ_0 in the composition range, X_{MeOH} from 0.6 to 0.8. The dielectric relaxation time had fairly large

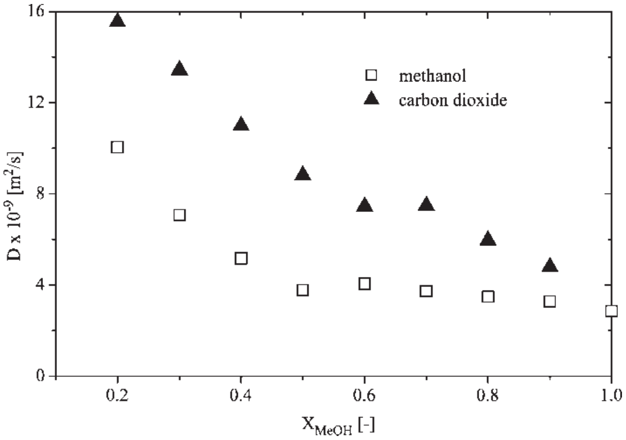

FIGURE 6 Simulation results of self-diffusion coefficients of methanol and carbon dioxide at 50°C. See Table III for densities.

discrepancies between experimental and simulated values for large methanol mole fractions. This is to be expected since the dielectric relaxation is a large-scale phenomenon and is not quantitatively represented in this work as a limited scale MD simulation.

From these results, we conjectured structure of methanol and CO_2 mixture. At X_{MeOH} of 1.0, methanol molecules make large hydrogen bond networks. When CO_2 was added to pure methanol, CO_2 existed in the hydrogen bond networks and the networks were remaining around X_{MeOH} of 0.6–0.8. This might cause the methanol self-diffusion coefficient not to change. The dielectric relaxation time increased with an increase in the interaction between methanol hydrogen bond networks via the presence of CO_2 molecules. Further addition of CO_2 into methanol caused the hydrogen bond networks to break up and to form smaller hydrogen bond aggregates. This probably causes an increase in self-diffusion coefficient and a decrease in relaxation time.

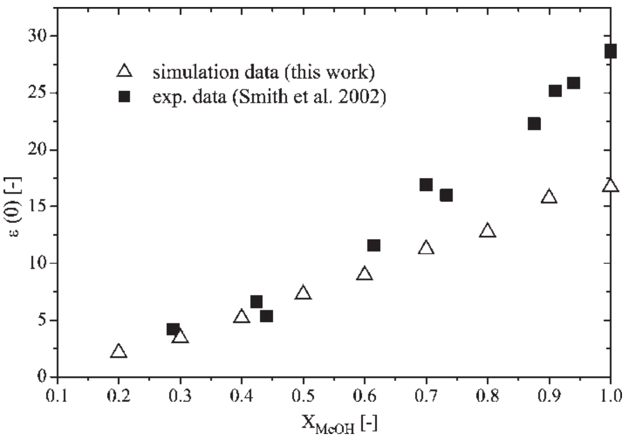

FIGURE 7 Static dielectric constant simulation (50°C) compared with experimental data (50°C, 11 MPa [7]). See Table III for densities.

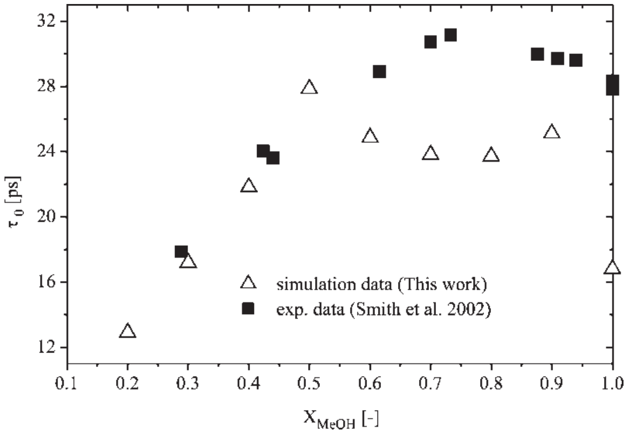

FIGURE 8 Relaxation time simulation (50°C) compared with experimental data (50°C, 11 MPa [7]). See Table III for densities.

CONCLUSIONS

MD simulations were made on methanol and CO_2 mixtures to examine some of the solution structural features of the expanded liquid state of methanol in terms of the RDF, self-diffusion coefficient and dielectric properties. From RDF results, the effect of CO_2 on nearest methanol hydrogen bond pairs occurred around X_{MeOH} of 0.6 and the tendency of both methanol and CO_2 self-diffusion coefficients were changed at this composition. This probably means that the methanol hydrogen bond networks change greatly around this composition. Simulation of dielectric relaxation time showed the possible existence of a maximum point in the composition range, X_{MeOH} from 0.6 to 0.8 in agreement with the experimental data.

Acknowledgements

This research was partially supported by the Ministry of Education, Culture, Sports, Science and Technology, a Grant-in-Aid for the COE project, Giant Molecules and Complex Systems and CREST of JST.

References

[1] Brunner, E., Hultenschmidt, W. and Schlichtharle, G. (1987) "Fluid mixtures at high-pressures. 4. Isothermal phase-equilibria in binary-mixtures consisting of (methanol + hydrogen or nitrogen or methane or carbon-monoxide or carbon-dioxide)", *J. Chem. Thermodyn.* **19**, 273–291.

[2] Wen, D. and Olesik, S.V. (2001) "Chromatography of ionizable positional isomers with methanol–water–carbon dioxide mixtures", *Anal. Chem. Acta* **449**, 211–220.

[3] Erkey, C. (2000) "Supercritical carbon dioxide extraction of metals from aqueous solutions: a review", *J. Supercritical Fluid* **17**, 259–287.

[4] Mingotaud, A.F., Bègue, G., Cansell, F. and Gnanou, Y. (2001) "Free-radical polymerization of styrene in CO2/ethanol mixed supercritical fluid", *Macromol. Chem. Phys.* **202**, 2857–2863.

[5] Matsuyama, K., Mishima, K., Hayashi, K., Ishikawa, H., Matsuyama, H. and Harada, T. (2003) "Formation of

microcapsules of medicines by the rapid expansion of a supercritical solution with a nonsolvent", *J. Appl. Polym. Sci.* **89**, 742–752.

[6] Reighard, T.S., Lee, S.T. and Olesik, S.V. (1996) "Determination of methanol/CO2 and acetonitrile/CO2 vapor–liquid phase equilibria using a variable-volume view cell", *Fluid Phase Equilib.* **123**, 215–230.

[7] Smith, R.L., Jr., Saito, C., Suzuki, S., Lee, S.B., Inomata, H. and Arai, K. (2002) "Temperature dependence of dielectric spectra of carbon dioxide and methanol mixtures at high-pressures", *Fluid Phase Equilib.* **194–197**, 869–877.

[8] Honma, T., Liew, C.C. and Inomata, H. (2003) "Flexible molecular model of methanol for a molecular dynamics study of liquid and supercritical conditions", *J. Phys. Chem. A* **107**, 3960–3965.

[9] Tuckerman, M.E. and Langel, W. (1994) "Multiple time scale simulation of flexible model of CO_2", *J. Chem. Phys.* **100**, 6368–6371.

[10] Toukan, K. and Rahman, A. (1985) "Molecular-dynamics study of atomic motions in water", *Phys. Rev. B* **31**, 2643–2648.

[11] Eyring, H., Henderson, D. and Jost, W. (1971) *Physical Chemistry An Advanced Treatise* (Academic Press, New York) Vol. VIII B.

[12] Smith, R.L., Jr., Lee, S.B., Suzuki, S., Saito, C., Inomata, H. and Arai, K. (2002) "Densities of carbon dioxide plus methanol mixtures at temperatures from 313.2 to 323.2 K and at pressures from 10 to 20 MPa", *J. Chem. Eng. Data* **47**, 608–612.

[13] Tuckerman, M., Berne, B.J. and Martyna, G.J. (1992) "Reversible multiple time scale molecular-dynamics", *J. Chem. Phys.* **97**, 1990–2001.

[14] Allen, M.P. and Tildesley, D.J. (1987) *Computer Simulation of Liquids* (Clarendon Press, Oxford).

[15] Böttcher, C.J.F. (1973) *Theory of Electric Polarisation* (Elsevier, Amsterdam).

[16] Yamaguchi, T., Hidaka, K. and Soper, A.K. (1999) "The structure of liquid methanol revisited: a neutron diffraction experiment at − 80°C and +25°C", *Mol. Phys.* **96**, 1159–1168.

[17] Yamaguchi, T., Hidaka, K. and Soper, A.K. (1999) "ERRATUM the structure of liquid methanol revisited: a neutron diffraction experiment at − 80°C and + 25°C", *Mol. Phys.* **97**, 603–605.

[18] Haughney, M., Ferrario, M. and Macdonald, I.R. (1987) "Molecular-dynamics simulation of liquid methanol", *J. Phys. Chem.* **91**, 4934–4940.

[19] Handgraaf, J.W., Erp, T.S. and Meijer, E.J. (2003) "*Ab initio* molecular dynamics study of liquid methanol", *Chem. Phys. Lett.* **367**, 617–624.

[20] Jorgensen, W.L., Maxwell, D.S. and Tirado-Rives, J. (1996) "Development and testing of the OPLS all-atom force field on conformational energetics and properties of organic liquids", *J. Am. Chem. Soc.* **118**, 11225–11236.

[21] Kosztolanyi, T., Bako, I. and Palinkas, G. (2003) "Hydrogen bonding in liquid methanol, methylamine, and methanethiol studied by molecular-dynamics simulations", *J. Chem. Phys.* **118**, 4546–4555.